ISSN 0038-0946, Solar System Research, 2021, Vol. 55, No. 5, pp. 402–408. © Pleiades Publishing, Inc., 2021.
Russian Text © The Author(s), 2021, published in Astronomicheskii Vestnik, 2021, Vol. 55, No. 5, pp. 408–415.

Results of Photometric Observations of Comet P/2019 LD2 at the Sanglokh Observatory

G. I. Kokhirova[a], *, F. J. Rakhmatullaeva[a], and S. A. Borisenko[b]

[a] *Institute of Astrophysics, National Academy of Sciences of Tajikistan, Dushanbe, Tajikistan*
[b] *Main Astronomical Observatory, National Academy of Sciences of Ukraine, Kyiv, Ukraine*
**e-mail: kokhirova2004@mail.ru*

Received March 29, 2021; revised June 3, 2021; accepted June 19, 2021

Abstract—The short-period comet P/2019 LD2 (Atlas) was discovered in June 2019. The object was originally classified as a Trojan asteroid, but was later included in the Jupiter family of comets. In view of the unknown nature of the object's origin, the study of the comet is of particular scientific interest. In this regard, optical observations of the comet were carried out in August 2020 at the Sanglokh International Astronomical Observatory (IAOS) of the Institute of Astrophysics of the National Academy of Science of Tajikistan. The magnitude of the absolute brightness of the comet in the filter R according to our measurements is 11.41^m, the dust production parameter and the upper limit of the core radius are estimated at 7.4 km. The distribution of brightness along the tail and dust tail structure were found. It is shown that the largest dust particles with a size of more than 100 μm are located near the surface of the comet's nucleus, and the size of the tail particles decreases with distance from the nucleus. Photometric data indicate that during the monitoring period, the comet was in a state of normal cometary activity, associated mainly with the recent passage of perihelion. An analysis of the comet's orbit showed that it is indeed in the transition from the centaur group to a comet of the Jupiter family.

Keywords: comet, photometry, brightness, dust production, radius, isophote, Finson–Probstein diagram
DOI: 10.1134/S0038094621050038

INTRODUCTION

The new short-period comet P/2019 LD2 (Atlas) was discovered on June 10, 2019, as part of the ATLAS robotic astronomical survey, performed in Hawaii in the United States. After processing the first images, the new faint asteroid-like object was classified as a Trojan asteroid of Jupiter (http://www.ifa.hawaii.edu/info/press-releases/2019LD2/, 2021). Trojan asteroids are two large groups of asteroids that move in the vicinity of two Lagrange singular points L_4 and L_5 of Jupiter's orbit in an orbital resonance of 1 : 1. It is believed that billions of years ago, Trojan asteroids clustered in these areas under the influence of Jupiter's gravity. However, subsequent observations showed that the object has signs of cometary activity – a faint coma and tail. As a result, it was declared the first Trojan asteroid of Jupiter to exhibit cometary activity (http://www.ifa.hawaii.edu/info/press-releases/2019LD2/, 2021). Later, more detailed observations, covering a large arc of the object's orbit, and careful processing of high-quality images, showed that 2019 LD2 is not in an orbital resonance 1 : 1 with Jupiter, as expected for a Trojan asteroid (MPEC 2020-K134: Comet P/2019 LD2 (ATLAS), 2020). Moreover, these observations confirmed that cometary activity became more noticeable and did not stop over time. Based on this, it was concluded that in fact this object is a comet of the Jupiter family with a chaotic orbit, temporarily captured by Jupiter from the centaur population and periodically approaching the gas giant, and in the work of Licandro et al. (2020) it has been suggested that P/2019 LD2 is a captured interstellar comet. So, initially 2019 LD2 was mistaken for a Trojan, but later it was identified as a comet of the Jupiter family. In this regard, the IAU Minor Planet Center has assigned the object a new designation P/2019 LD2 (ATLAS) in accordance with the rules of the cometary nomenclature (MPEC 2020-K134: Comet P/2019 LD2 (ATLAS), 2020).

Orbital elements of P/2019 LD2 are given in Table 1 (MPEC2020-K134: Comet P/2019 LD2 (ATLAS), 2020), where a is the semimajor axis, e is the eccentricity, q and Q are the perihelion and aphelion distances, respectively, i is the inclination, ω is the perihelion argument, and Ω is the longitude of the ascending node. The comet revolves around the Sun at an average distance of 5.28 AU. That is, every 12.12 years. The orbit has an eccentricity of 0.132 and an inclination of 11.6° with respect to the ecliptic, the Tisserand parameter is 2.94, which is typical for the orbits of other comets of the Jupiter family. The comet's nominal orbit assumes that it is not in a stable resonance 1 : 1

Table 1. Orbital elements of comet P/2019 LD2 (Atlas) (J2000.0)

Epoch	a, AU	e	q, AU	Q, AU	i, deg	ω, deg	Ω, deg
31.05.2020	5.295	0.135	4.578	6.013	11.552	123.448	179.746

with Jupiter, since on February 17, 2017, it came close to the planet at a distance of 0.092 AU (13.8 million km) and will make the same close approach in 2028 (JPL Small-Body Database Browser: P/2019 LD2, 2020). The comet passed the next perihelion of its orbit on April 10, 2020 (P/2019 LD2, MPC IAU, 2020).

The absolute brightness of the comet $H = 12.1–12.2^m$ (P/2019 LD2, MPC IAU, 2020; JPL Small-Body Database Browser: P/2019 LD2, 2020), the diameter is estimated at about 14 km with an assumed albedo for this class of objects of 0.12 (Fernandez et al., 2009). The period of rotation and the geometric shape of the nucleus need to be clarified.

The orbit of the new comet is partially within the orbit of Jupiter, its activity resembles that of comet 29P/Schwasman-Wachman 1, belonging to the group of centaurs. Note that Sarid et al. (2019) consider object 29P to be the prototype "gateway" between centaurs and comets of the Jupiter family. In this context, the study of P/2019 LD2 contributes to a better understanding of the peculiarities of the transition from centaurs to comets of the Jupiter family. If it turns out that P/2019 LD2 is an interstellar comet, then it becomes possible to study this class of objects. This explains the relevance of observations and studies of the new comet.

OBSERVATIONS AND DATA PROCESSING

In order to study the new comet, we carried out photometric observations of the object at the Sanglokh International Astronomical Observatory (IAOS) of the Institute of Astrophysics of the National Academy of Sciences of Tajikistan using the Zeiss-1000 telescope. The object was registered using a FLI Proline PL16803 (4096 × 4096 pixels, pixel size 9 μm). Readout noise of the camera is 10 e^- (electrons), the calculated conversion factor (gain) is about 0.497 e^-/ADU (analog to digital units). The camera was installed at the Cassegrain focus of the telescope (13 300 mm) and equipped with standard broadband photometric filters of the Johnson–Cousins system allowing us to select the appropriate range of the spectrum during observations. To increase the signal-to-noise ratio (S/N) of the images, 4 × 4 binning was used. As a result, the scale of the images was 0.579"/pixel with a field of about 10′ × 10′. To reduce the noise level of the CCD camera, the CCD matrix is cooled to a temperature of −20°C.

Primary processing (accounting for dark currents, bayesian and flat fields) and image addition was carried out using Astroart 4.0 software (http://www.msb-astroart.com/, 2021). For aperture photometry of the comet and reference stars, we used the ATV utility under IDL for Windows (Barth, 2001).

The APASS catalog (DR9) (Henden et al. 2016) was used to identify the reference stars. The catalog includes stars up to about magnitude 17 in filters B and V, as well as in special cometary filters of the Sloane system g', r', i'. The brightness of the catalog stars was determined with an accuracy of 0.07^m for band B, 0.05^m for band V and less than 0.03^m for band r' (Henden et al., 2016). For the transition from magnitudes in the band r' to the values in the band Rc the formula from (Munari et al., 2014) was used. Photometric standards of 5–7 stars of stellar magnitude 13–17 were selected for each night of observations using the Aladin online service (http://www.aladin.u-strasbg.fr, 2021).

RESULTS AND PHYSICAL PROPERTIES

A summary of observations during five nights in August 2020 and the results of photometric processing are given in Table 2. The position of the comet's orbit during monitoring is indicated here: r and Δ are the distance of the comet from the Sun and the Earth, ph is the phase angle, data taken from the MRS database (https://www.minorplanetcenter.net, 2020), details of the exposures performed: N_R and t are the number and time of exposures in the filter R, averaged apparent magnitudes m_R at the time of exposure and absolute magnitude $m_R(1,1,0)$ of the object obtained in the filter R, as well as estimates of the dust production parameter $Af\rho$ and radius r_N of the comet nucleus according to our measurements. Image measurements were performed with an aperture radius ρ = 4.05″, the projection of which on the plane of the object corresponds to 10 588 km, the last value is calculated by the ratio ρ = Δtan (ρ). The radius of the aperture for measuring the brightness of the comet was determined using growth curves using Astroart and corresponds to the maximum signal-to-noise ratio (SNR). The image of the comet during observations is shown in Fig. 1.

As may be seen from Table 2, during the monitoring period, the apparent brightness of the comet did not undergo significant changes. Apparent brightness m_R converted to absolute brightness of the comet's nucleus $m_R(1,1,0)$ using the following empirical equation (Snodgrass et al., 2014) gives:

$$m_R(1,1,0) = m_R - 5\log(r\Delta) - \beta\alpha, \quad (1)$$

here $m_R(1,1,0)$ is the the brightness of a hypothetical point at unit heliocentric and geocentric distances

Table 2. Ephemeris data of comet P/2019 LD2 (Atlas) during observations in 2020 and results of photometric measurements

Date, UT	r, AU	Δ, AU	ph, deg	$N_R \times t$, s	m_R, stellar magnitude	$Af\rho$, cm	ρ, arc s	$m_R(1,1,0)$, stellar magnitude	r_N, km
August 6 17:03:33	4.591	3.590	2.3	28 × 120	17.53 ± 0.03	272 ± 7.5	4.05	11.41 ± 0.03	7.4 ± 0.14
August 7 17:31:26	4.591	3.590	2.3	41 × 120	17.54 ± 0.04	269 ± 9.9			
August 8 16:59:45	4.592	3.590	2.2	23 × 120	17.71 ± 0.04	230 ± 8.5			
August 14 21:43:15	4.593	3.597	2.6	24 × 120	17.58 ± 0.02	260 ± 4.8			
August 15 20:36:11	4.593	3.599	2.7	53 × 120	17.62 ± 0.01	251 ± 2.3			

with a phase angle $ph = 0$ deg, m_R is the measured brightness, r and Δ are the heliocentric and geocentric distances of the comet in AU, i.e., α is the phase angle (ph) in degrees, β is the phase coefficient in magnitudes per degree. For the phase coefficient, the generally accepted value β = 0.04 stellar magnitudes/deg (Lamy et al., 2004). According to our measurements, the absolute brightness of the comet was 11.41^m (Table 2), its difference from the ephemeris value at a unit heliocentric distance is $12.1-12.2^m$ indicates the object's normal cometary activity during this period.

Isophotes of the comet, built using SAO Image DS9 (https://sites.google.com/cfa.harvard.edu/saoimageds9, 2021) are shown in Fig. 2 and clearly demonstrate the brightness distribution along the comet's tail.

The upper limit of the radius of the cometary nucleus at the moment of minimum activity over the

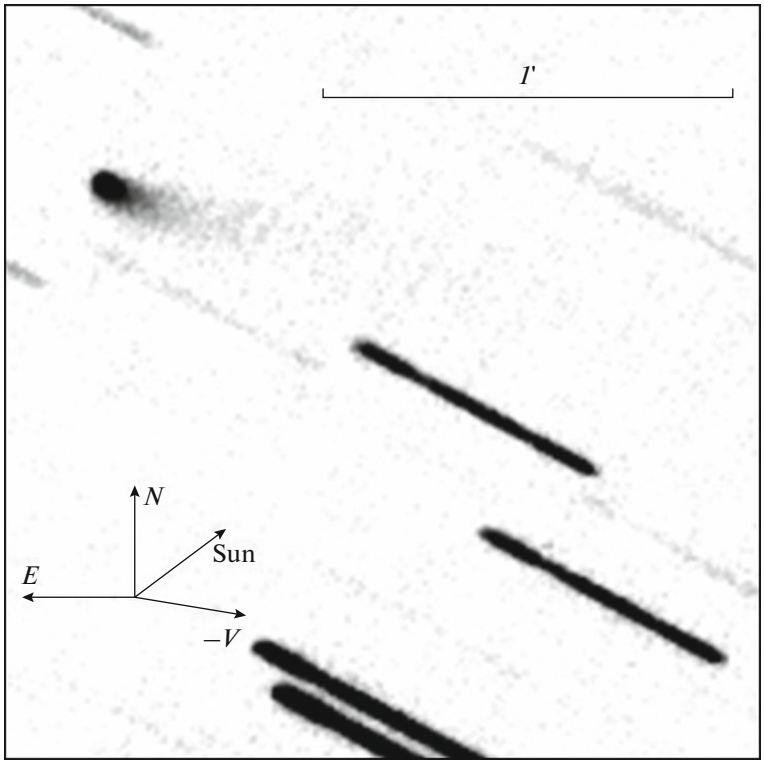

Fig. 1. Filter summary of comet P/2019 LD2 in filter *R*, August 15, 2020, telescope Zeiss-1000 MAOS.

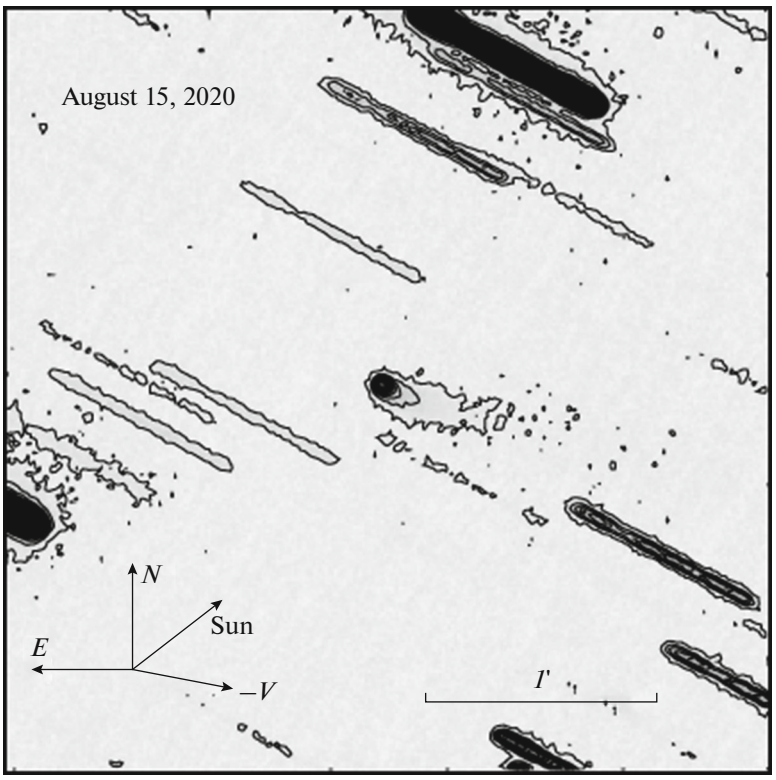

Fig. 2. Image of the comet's tail taken on August 15, 2020. Isophotes were used to improve the visibility of the tail.

observation period, which, judging by the value of the dust production parameter, fell on August 8, 2020, was estimated using the following empirical relationship between the absolute brilliance $m_R(1,1,0)$ of the comet measured in the R filter and the effective radius of the comet nucleus r_N in meters (see, for example, Solontoi et al., 2012)

$$A_R r_N^2 = 2.238 \times 10^{22} \times 10^{0.4(m_\odot - m_R(1,1,0))}, \quad (2)$$

where A_R is the geometric albedo and $m_\odot = -27.29$ stellar magnitude, the apparent brightness of the Sun (Cox, 2000), with both values in the filter R. Estimation of the upper limit of the radius of the core obtained using the albedo value for cometary dust $A_R = 0.12$ (Fernandez et al., 2009), is 7.4 km (Table 2) and is consistent with a core diameter of 14 km, given in various databases.

DUST PRODUCTIVITY OF THE COMET

The comet's activity level can be quantified using the parameter $Af\rho$, which is theoretically independent of the time and place of observation (A'Hearn et al., 1984). Parameter $Af\rho$ can be determined by magnitude using the following expression (A'Hearn et al. 1984):

$$Af\rho = \frac{4r^2\Delta^2 10^{0.4(m_\odot - m_a)}}{\rho}, \quad (3)$$

where A is the albedo, f is the filling factor of the aperture of the field of view corresponding to cometary dust, ρ is the projection of the radius of the photometric aperture onto the plane of the sky in cm, $m_\odot$ and m_a are the apparent stellar magnitudes of the Sun and comets, respectively, in a certain filter, r is the heliocentric distance of the object in AU and Δ the geocentric distance in cm. For observations made with the Zeiss-1000 telescope, the parameter $Af\rho$ is calculated using images obtained in the filter R, and the same radius of the projection of the aperture ρ = 10 588 km (4.05"). The values together with errors are shown in Table 2. The values of the dust production parameter above 100 cm, along with the magnitude of the absolute brightness, also confirm the increased activity of the comet (Hicks et al., 2007). In addition, during the observation period, the heliocentric distance gradually increased; in this regard, there is a tendency for the parameter to decrease.

Figure 3 shows the distribution of the parameter $Af\rho$ as a function of the radius of the measurement aperture, found from our observations.

DUST TAIL STRUCTURE

The motion of dust particles in a cometary tail is a complex process, and an accurate description of the trajectories of particles in the cometary atmosphere requires improved hydrodynamic models that take

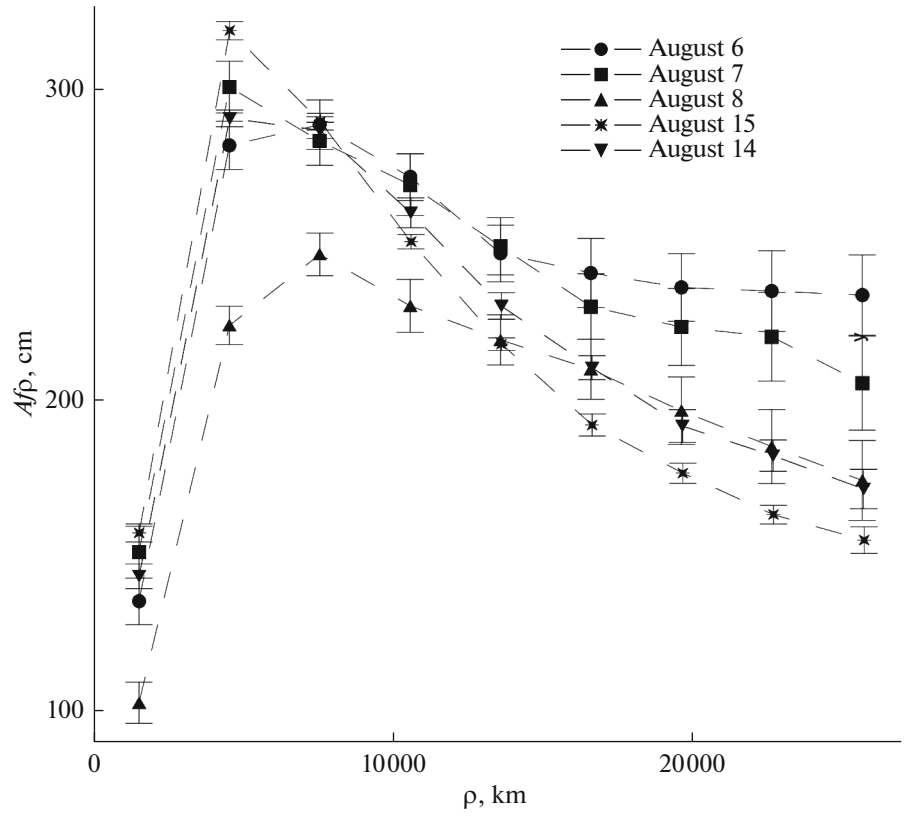

Fig. 3. Parameter distribution of $Af\rho$ depending on the radius of the photometric aperture.

into account the interaction between gas and dust released from the surface. In a cometary tail, dust and gas are separated, and the only significant forces affecting the trajectory of particles are solar gravity and radiation pressure. Both forces depend on the square of the heliocentric distance, but act in opposite directions. The equation of motion in this case can be represented as:

$$m \times a = (1 - \gamma) g_{\text{Sun}}, \quad (4)$$

where m and a are the mass and acceleration of the dust particle, respectively, γ is the ratio of the radiation pressure and the solar acceleration of gravity ($\gamma = P_{\text{radiation}}/g_{\text{Sun}}$), which is inversely proportional to the size for particles larger than 1 μm (Finson and Probstein, 1968). Based on this relationship, Finson and Probstein (1968) proposed a model that describes the complete geometry of the tail with a grid of synchro and sindinam lines representing, respectively, the locations of particles ejected from the surface of the nucleus at the same time or with the same γ parameter.

The Finson–Probstein model is simplified because it considers only particles ejected in the comet's orbital plane and with zero initial velocity, but it provides a very good approximation of the tail shape and has been successfully used to study the tails of both comets and some active asteroids (Borysenko et al., 2020a).

We have built a Finson–Probstein diagram of the comet's tail using the Internet service (http://www.comet-toolbox.com/FP.html, 2021) and elements of the comet's orbit according to MPC data (MPEC 2020-UR0, 2021) (Figs. 4a, 4b). On the diagram, the coordinates of the comet are plotted along the abscissa and ordinate axes, right ascension α and declination δ, respectively. Figure 4a shows the distribution of synchro and sindinam in the inner sector of the tail (region size approximately 13" × 13"). Their distribution over the entire visible part of the cometary tail is shown in Fig. 4b (the size of the region is approximately 108" × 108"). Considering that $\gamma = 0.57Q_{\text{pr}}/\sigma a$, where σ is the dust grain density, expressed in g/cm^3, a is the dust particle radius in μm, Q_{pr} is the radiation pressure efficiency, which depends on the size, shape and optical characteristics of the dust grain (for cometary dust, the radiation pressure efficiency is usually of the order of unity), then, taking the density of cometary dust to be about 0.1 g/cm^3 (Greenberg and Li, 1999), it can be said that large particles >100 μm in size are dominant in the inner regions of the comet's tail.

The presence of a short tail in the opposite direction of the comet's motion indicates the presence of coarse-grained dust in the cometary atmosphere. The solar wind hardly acts on cometary dust, it is pushed

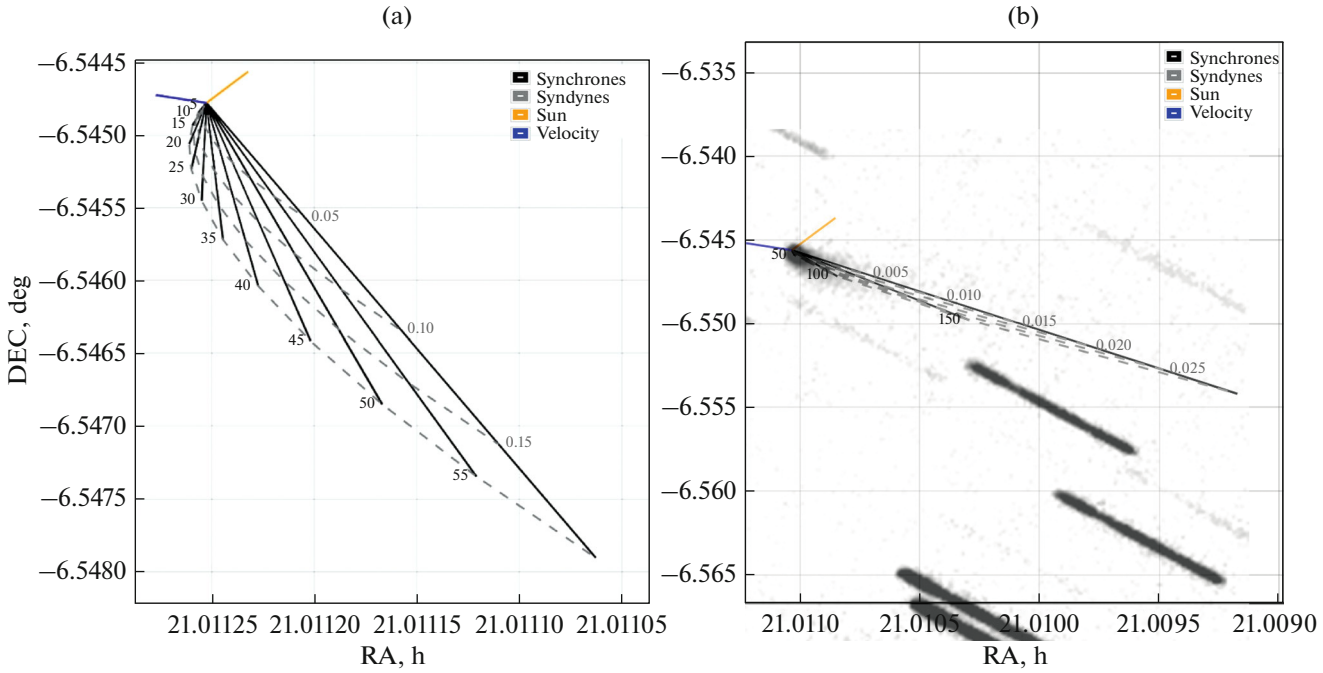

Fig. 4. (a) Finson–Probstein diagram for the tail of comet P/2019 LD2 (ATLAS) (inner sector), August 15, 2020, syndynes (dashed lines) show the distribution of γ for comet dust particles (γ = 0.05; 0.1; 0.15), which is inversely proportional to their size; synchrones (solid lines) show the geometrical place of dust grains of various sizes, which were released from the core a certain time ago (d = 5–60 days) from the moment of observation. Directions to the Sun and velocity vectors are also shown in the diagram. (b) Finson–Probstein plot of the P/2019 LD2 tail overlaid on a grid in real scale as of August 15, 2020, showing the distribution of sindins and synchro across the entire visible part of the tail.

out of the coma by the pressure of sunlight. Therefore, the formation of the tail is determined by the initial orbital speed of movement and the acceleration under the influence of light pressure.

CONCLUSIONS

Based on data from photometric observations of comet P/2019 LD2 (ATLAS) conducted over five nights in August 2020 with the Zeiss-1000 telescope at Sanglokh Observatory using a broadband filter *R,* the physical characteristics of the comet were obtained:

(1) Apparent magnitudes m_R by measurements of each night of observations.

(2) Absolute magnitude $m_R(1,1,0) = 11.42^m$.

(3) Parameter of dust production $Af\rho$ about 250 cm (at ρ = 4.05″).

(4) Estimate of the upper limit of the radius of the comet's nucleus r_{max} = 7.4 km at albedo A = 0.12.

(5) Isophotes of the comet were constructed, demonstrating the distribution of brightness along the tail.

(6) Finson–Probstein diagrams of the inner and all visible part of the comet's dust tail were constructed and its structure, namely the distribution of dust particles by size and by the time of ejection from the surface of the nucleus, was found. It was shown that large particles over 100 μm in size are dominant in the inner regions of the dust tail.

(7) Photometric data indicate that during the monitoring period the comet was in a state of slightly increased cometary activity, associated mainly with the recent passage of the perihelion. During the observations, the comet's heliocentric distance was 4.591–4.593 AU. At such distances, less than the so-called "snow line" (Jewitt et al., 2007), to some extent, the typical actions responsible for normal cometary activity can still manifest themselves, namely, solar heating of the surface, sublimation of surface frozen volatile components, dust emission and the formation of a coma and tail. These findings support the findings of Sarid et al. (2019), who showed that the region of the location of transit objects (from centaurs to comets of the Jupiter family), to which, along with comet 29P, P/2019 LD2 (ATLAS) belongs, coincides with the heliocentric range of distances, where the activity of the observed cometary bodies significantly increases.

(8) The comet's current orbit indicates that the comet is in the transition from centaurs to comets of the Jupiter family. A slightly increased value of $Af\rho$ compared with other comets of the Jupiter family (Borysenko et al., 2019; 2020b) may indicate a previous long stay of the comet in the outer regions of the solar system.

REFERENCES

A'Hearn, M.F., Schleicher, D.G., Millis, R.L., Feldman, P.D., and Thompson, D.T., Comet Bowell 1980b, *Astron. J.,* 1984, vol. 89, pp. 579–591.

Aladin Sky Atlas, 2021. http://www.aladin.u-strasbg.fr.

Astroart 7. Astrophotography Suite, 2021. http://www.msb-astroart.com/.

Barth, A., ATV: An image-display tool for IDL, in *ASP Conf. Ser., Astron. Data Analysis Software and Systems X,* Harnden, F.R., Jr., Primini, F.A., and Payne, H.E, Eds., San Francisco: ASP, 2001, vol. 238, p. 385.

Borysenko, S., Baransky, A., and Musiichuk, E., Photometric observations of ecliptic comet 47p/Ashbrook-Jackson and selected quasi-Hilda and main-belt comets at Kyiv Comet Station (MPC code-585) in 2017, *Icarus,* 2019, vol. 317, pp. 44–47.

Borysenko, S., Baransky, A., Simon, A., and Vasylenko, V., Broadband photometry of asteroid 6478 Gault: Activity and morphology, *Astron. Nachrichten,* 2020a, vol. 341, no. 4, pp. 395–401.

Borysenko, S., Baransky, A., Kuehrt, E., Hellmich, S., Mottola, S., and Meech, K., Study of the physical properties of selected active objects in the main belt and surrounding regions by broadband photometry, *Astron. Nachrichten,* 2020b, vol. 341, no. 9, pp. 849–859.

Comet-Toolbox. Finson–Probstein diagram, 2021. http://www.comet-toolbox.com/FP.html.

Cox, A.N. and Pilachowski, C.A., Allen's astrophysical quantities, *Phys. Today,* 2000, vol. 53, p. 77.

Fernandez, Y.R., Jewitt, D., and Ziffer, J.E., Albedos of small Jovian Trojans, *Astron. J.,* 2009, vol. 138, no. 1, pp. 240–250.

Finson, M.L. and Probstein, R.F., A theory of dust comets. I. Model and equations, *Astron. J.,* 1968, vol. 154, pp. 353–380.

Greenberg, J.M. and Li, A., Morphological structure and chemical composition of cometary nuclei and dust, *Space Sci. Rev.,* 1999, vol. 90, pp. 149–161.

Henden, A.A., Templeton, M., Terrell, D., Smith, T.C., Levine, S., and Welch, D., VizieR online data catalog: AAVSO photometric all sky survey (APASS) DR9 (Henden+, 2016), *VizieR Online Data Catalog,* 2016, II-336.

Hicks, M.D., Bambery, R.J., Lawrence, K.J., and Kollipara, P., Near-nucleus photometry of comets using archived NEAT data, *Icarus,* 2007, vol. 188, pp. 457–467.

Institute for Astronomy, University of Hawaii. UH ATLAS telescope discovers first-of-its-kind asteroid. https://www.ifa.hawaii.edu/info/press-releases/2019LD2//. Accessed February 2021.

Jet Propulsion Laboratory. JPL Small-Body Database Browser: P/2019 LD2 (2020-05-19 last obs.). https://www.ssd.jpl.nasa.gov/. Accessed February 2021.

Jewitt, D., Chizmadia, L., Grimm, R., and Prialnik, D., Water in the small bodies of the Solar System, in *Protostars and Planets V,* Reipurth, B., Jewitt, D., and Keil, K., Eds., Tucson: Univ. Arizona Press, 2007, pp. 863–878.

Lamy, P.L., Toth, I., Fernandez, Y.R., and Weaver, H.A., *The sizes, shapes, albedos, and colors of cometary nuclei, Comets II,* Festou, M.C., Keller, H.U., and Weaver, H.A., Eds., Tucson: Univ. Arizona Press, 2004, pp. 223–264.

Licandro, J., Pinilla-Alonso, N., de Leon, J., Moreno, F., et al., Observations of Comet P/2019 LD2 (ATLAS) with the 10-m Gran Telescopio Canarias (GTC), *AAS Division of Planet. Sci. Meeting, Bull. Am. Astron. Soc.,* 2020, vol. 52, no. 6, id. 404.06.

Minor Planet Center. Minor Planet & Comet Ephemeris Service, 2020. https://www.minorplanetcenter.net/iau/MPEph/MPEph.html.

Minor Planet Center. P/2019 LD2. https://www.minorplanetcenter.net. Accessed February 2021.

Minor Planet Electronic Circular. MPEC 2020-K134: COMET P/2019 LD2 (ATLAS). https://www.minorplanetcenter.net/mpec/K20/K20KD4.html. Accessed February 2021.

Minor Planet Electronic Circular. MPEC 2020-UR0. https://www.minorplanetcenter.net. Accessed February 2021.

Munari, U., Henden, A., Frigo, A., and Dallaporta, S., APASS discovery and characterization of 180 variable stars in Aquarius, *J. Astron. Data,* 2014, vol. 20, p. 4.

Russell, H.N., On the albedo of the planets and their satellites, *Astrophys. J.,* 1916, vol. 43, pp. 173–196.

SAOImageDS9, 2021. https://sites.google.com/cfa.harvard.edu/saoimageds9.

Sarid, G., Volk, K., Steckloff, J.K., et al., 29P/Schwassmann–Wachmann 1, a Centaur in the gateway to the Jupiter-family comets, *Astrophys. J. Lett.,* 2019, vol. 883, no. 1, art. id. L25.

Snodgrass, C., Lowry, S.C., and Fitzsimmons, A., Photometry of cometary nuclei: rotation rates, colours and a comparison with Kuiper Belt Objects, *Mon. Not. R. Astron. Soc.,* 2006, vol. 373, pp. 1590–1602.

Solontoi, M., et al., Ensemble properties of comets in the Sloan Digital Sky Survey, *Icarus,* 2012, vol. 218, pp. 571–584.

Vincent, J.-B., Comet-toolbox: Numerical simulations of cometary dust tails in your browser, in *Asteroids, Comets, Meteors 2014. Proc. Conf. (Helsinki, 2014),* Muinonen, K., et al., Eds., 2014, p. 565V.